Vygotsky: Jurnal Pendidikan Matematika dan Matematika
8 (2) August 2026, pp. 115 - 126
E-ISSN: 2656-5846 P-ISSN: 2656-2286
Journal Page is available to
https://jurnalpendidikan.unisla.ac.id/index.php/VoJ

Modeling and Design of LTV-MPC Controller for Palm Sap Bioreactor System

Aisyah Fikriyah Zahirah[1], Dia Ayu Nazihah[1], Ni Luh De Siska Sari Dewi[1], Arief Abdurrakhman[2], Mardlijah Mardlijah[1*]

[1] Department of Mathematics, Institut Teknologi Sepuluh Nopember, Indonesia
[2] Department of Instrumentation Engineering, Institut Teknologi Sepuluh Nopember, Indonesia

Email Correspondence: mardlijah@its.ac.id

ARTICLE INFO

Article History

Received	:	23 Apr 2026
Revised	:	14 Aug 2026
Accepted	:	21 Aug 2026
Available Online	:	31 Aug 2026

Keywords:
Mathematical Modelling
Control Optimal
LTV-MPC
Temperature Dynamics
Pressure Dynamics

Please cite this article APA style as:
Zahirah, A. F., Nazihah, D. A., Dewi, N. L. D. S. S., Abdurrakhman, A., & Mardlijah, M. (2026). Modeling and Design of LTV-MPC Controller for Palm Sap Bioreactor System. *Vygotsky: Jurnal Pendidikan Matematika dan Matematika*, 8(2), pp. 115-126.

ABSTRACT

Bioethanol production's nonlinear thermodynamic dynamics risk yeast damage and overpressure. This study designs a Linear Time-Varying Model Predictive Control (LTV-MPC), whose model is governed by the laws of mass and energy conservation, to simultaneously control juice temperature and pressure in a bioreactor. Using successive linearization, actuator rate limits are integrated to dampen thermal lag. Solved via Quadratic Programming, the LTV-MPC successfully stabilizes pressure at 145 psi by adaptively sacrificing the $50^{\circ}C$ temperature target to prevent critical limit violations. Evaluations demonstrate the system's robustness in ensuring operational safety and minimizing explosion risks.

Vygotsky: Jurnal Pendidikan Matematika dan Matematika with CC BY NC SA license
Copyright © 2026, The Author (s)

1. Introduction

The sugar palm tree (Arenga pinnata) has high economic potential in Indonesia, primarily through its sap, which contains over 10% sucrose and low alcohol content (Dewi et al., 2024; Hutami et al., 2023). This chemical composition makes sugar palm sap a potential first-generation bioethanol feedstock to address the drastic decline in national oil reserves since 2010 (Krisnanto et al., 2025). As a new and renewable energy (NRE) source, bioethanol is environmentally friendly with lower emissions compared to fossil fuels (Khairiah & Ridwan, 2021; Rifa'i et al., 2022; Wilberta et al., 2021). However, the competitiveness of bioethanol in the

E-ISSN: 2656-5846
P-ISSN: 2656-2286

domestic market is still hindered by high production costs compared to subsidized gasoline, necessitating production process efficiency to reduce this price gap (Deloitte Consulting Southeast Asia, 2023; Dewi et al., 2026).

Bioethanol production efficiency is significantly determined by the fermentation stage, which generates massive heat (exothermic) and CO_2 gas (Salazar et al., 2023). At a small scale, equipment limitations complicate temperature management and trigger back-pressure. Failure to control these two factors can inhibit fermentation performance while compromising the physical safety of the reactor (Nadal-Rey et al., 2021).

Previous studies have identified limitations in thermal bioreactor control under coupled thermodynamic and hydrodynamic constraints. Conventional Proportional-Integral-Derivative (PID) controllers often struggle with multivariable systems and limited cooling capacity, lacking predictive constraint handling and risking temperature overshoot and overpressure. (Ameliyah & Arif, 2026). Conversely, optimal control approaches such as Pontryagin's Minimum Principle (PMP) require highly complex explicit biological models that are computationally demanding and difficult to implement in real-time systems (Darajat et al., 2023). Furthermore, standard Model Predictive Control (MPC) based on Linear Time-Invariant (LTI) frameworks assumes constant system parameters, potentially causing plant-model mismatch under fluctuating heat generation and gas production during fermentation. This limitation highlights the need for a constraint-aware control strategy that accommodates time-varying biological disturbances without requiring complex kinetic models. Accordingly, this study develops a Linear Time-Varying Model Predictive Control (LTV-MPC) strategy.

The novelty of this research lies in the development of a prioritized constraint-handling mechanism within the LTV-MPC framework, specifically designed to resolve conflicting thermodynamic and hydrodynamic constraints. Instead of a standard application, the algorithm integrates successive linearization and an augmented state-space formulation featuring strict actuator rate limits to dynamically enforce critical pressure boundaries, even if it requires adaptively sacrificing secondary temperature targets. The primary contributions of this research include the formulation of an integrated temperature and pressure dynamics model aligned with real instrumentation, as well as the design of an LTV-MPC capable of handling strict operational constraints. To validate its reliability, the proposed control strategy is subsequently evaluated under constant ambient temperature scenarios, aiming to ensure industrial safety and minimize overpressure risks.

2. Method

This research utilizes physical and thermodynamic parameters of a 50L bioethanol reactor to estimate the system matrix $A(t)$ and the input matrix $B(t)$. These parameters are then applied to simulate the model dynamics. The research procedure is conducted through systematic stages and is described as follows:

a. Mathematical Model Formulation
   Derived from mass and energy conservation laws, the mathematical model is formulated as a state-space system with four explicit state variables (Kumar et al., 2019). These variables comprehensively capture the thermal dynamics,

E-ISSN: 2656-5846
P-ISSN: 2656-2286

represented by palm sap temperature (T) and jacket temperature (T_j), and the hydrodynamic dynamics, denoted by reactor pressure (P_r) and gas storage tank pressure (P_g). To safely manage these coupled dynamics, the MPC algorithm explicitly regulates two manipulated control variables: heater power (u_h) and gas valve opening (u_v). This control action ensures the system tracks operational setpoints without violating critical physical boundaries. The physical design of this system is illustrated in Figure 1.

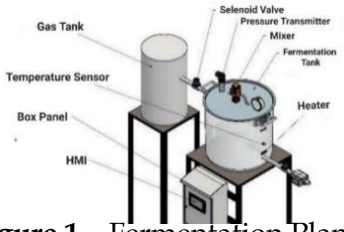


Figure 1. Fermentation Plant

b. Linearization of non-linear models using Taylor expansion (Jacobian) at each operating time.
c. System Structural Properties Analysis
   Before controller design is carried out, an analysis of the system's characteristics needs to be performed (Zhang et al., 2023):
   i. Stability analysis is performed using the state transition matrix $\Phi(t, t_0)$. This examines the system's error dynamics, where divergence indicates instability and convergence ensures stability.
   ii. Gaussian elimination verifies that both matrices achieve full rank, ensuring all internal states are controllable via inputs and observable from sensor outputs.
d. LTV-MPC Control Design
   This stage involves designing the control algorithm through the following steps
   i. Discretization by converting model to a discrete form using the Zero-Order Hold (ZOH) with sampling interval T_s.
   ii. Augmented Model Formulation by combining state variables with past actions to eliminate steady-state error (Zhang et al., 2025).
   iii. Constraints Formulation by defining physical limits for inputs, input rate of change (Δu), and safety output boundaries (Bujarbaruah et al., 2022; Ławryńczuk et al., 2022; Xu et al., 2026).
   iv. Weighting Matrix (Q and R) by balancing tracking performance and energy efficiency.
e. Simulation
   The algorithm was implemented in MATLAB to evaluate closed-loop performance. The final evaluation analyzed minute-by-minute computational data against setpoints of $50^{\circ}C$ for the bioreactor and jacket temperatures, and 145 psi for the reactor and gas storage tank pressures.

3. Results and Discussion

Mathematical modeling and open-loop LTV simulation are discussed in this section to analyze the impact of temperature and pressure fluctuations on the reactor's natural instability, which are then validated using thermodynamic principles and previous literature.

https://doi.org/10.30736/voj.v8i2.1367

E-ISSN: 2656-5846
P-ISSN: 2656-2286

3.1. Mathematical Modeling of Bioreactor Dynamics

The reactor temperature model is developed based on the heat balance of a jacketed reactor system, which consists of two main components:

3.1.2. Reactor Temperature ($\boldsymbol{T}$)

The reactor temperature model is developed based on the system's heat balance and the energy balance within the reactor:

Heat accumulation = heater input + heat of reaction – heat transfer to coolant.

$$m_r C_{p,r} \frac{dT}{dt} = Q_{in} + Q_{rxr} - Q_{out} \quad (1)$$

$$\frac{dT}{dt} = \frac{1}{m_r C_{p,r}} [Q_{in} + Q_{rxr} - Q_{out}]$$

The rate of heat transfer follows Newton's law of cooling.

$$Q_{out} = UA(T - T_j)$$

Substituting the equation above results in the reactor temperature dynamics model becoming,

$$\frac{dT}{dt} = \frac{1}{m_r C_{p,r}} \left[Q_{in} + Q_{rxr} - UA(T - T_j)\right]$$

$$\frac{dT}{dt} = \frac{1}{m_r C_{p,r}} \left[u_h(t) P_{heat} + Q_{rxr} - UA(T - T_j)\right] \quad (2)$$

3.1.2. Passive Cooling Temperature ($\boldsymbol{T_j}$)

The energy absorbed by the jacket from the reactor, which is partially dissipated to the environment through natural convection, is expressed as:

Heat accumulation in the coolant = heat from the reactor – heat released to the environment.

$$m_j C_{p,j} \frac{dT_j}{dt} = Q_{out} - k_{loss}(T_j - T_{amb})$$

$$\frac{dT_j}{dt} = \frac{1}{m_j C_{p,j}} \left[Q_{out} - k_{loss}(T_j - T_{amb})\right]$$

$$\frac{dT_j}{dt} = \frac{1}{m_j C_{p,j}} \left[UA(T - T_j) - k_{loss}(T_j - T_{amb})\right] \quad (3)$$

3.1.3. Reactor Pressure ($\boldsymbol{P_r}$)

The pressure model is formulated using the ideal gas law and the principle of mass balance in the reactor headspace. The accumulation of gas in the reactor is the difference between the CO_2 production rate and the discharge rate through the valve.

$$\frac{dP_r}{dt} = \frac{RT}{V_h}\left(F_{gas} - F_{out}\right) + \frac{P_r}{T}\frac{dT}{dt}$$

$$\frac{dP_r}{dt} = \frac{RT}{V_h}\left(F_{gas} - C_v u_v \sqrt{P_r - P_g}\right) + \frac{P_r}{T}\frac{dT}{dt} \quad (4)$$

3.1.4. Storage Tank Pressure ($\boldsymbol{P_g}$)

The accumulation of gas in the external tank is determined by the inflow rate from the reactor and can be written as follows:

$$V_t \frac{dP_g}{dt} = RT_{amb}(F_{out})$$

$$\frac{dP_g}{dt} = \frac{RT_{amb}}{V_t}(F_{out})$$

$$\frac{dP_g}{dt} = \frac{RT_{amb}}{V_t}\left(C_v u_v \sqrt{P_r - P_g}\right) \quad (5)$$

Based on this formulation, the system of differential equations representing the dynamics of bioethanol fermentation under the control scheme is expressed as

E-ISSN: 2656-5846
P-ISSN: 2656-2286

follows.

$$\begin{cases} \frac{dT}{dt} = \frac{1}{m_r C_{p,r}}\left[u_h(t)P_{heat} + Q_{rxr} - UA(T - T_j)\right] \\ \frac{dT_j}{dt} = \frac{1}{m_j C_{p,j}}\left[UA(T - T_j) - k_{loss}(T_j - T_{amb})\right] \\ \frac{dP_r}{dt} = \frac{RT}{V_h}\left(F_{gas} - C_v u_v\sqrt{P_r - P_g}\right) + \frac{P_r}{T}\frac{dT}{dt} \\ \frac{dP_g}{dt} = \frac{RT_{amb}}{V_t}\left(C_v u_v\sqrt{P_r - P_g}\right) \end{cases} \quad (6)$$

The parameters used in the system are defined as follows.

Table 1. Physical Parameters of The Bioreactor System Model

No.	Symbol	Definition	Value	Unit
1.	m_r	Mass of sap inside the reactor	40	Kg
2.	$C_{p,,r}$	Specific heat capacity of the sap	3900	J/(kg·K)
3.	m_j	Mass of fluid inside the thermal jacket	5	Kg
4.	$C_{p,j}$	Specific heat capacity of the jacket fluid	2100	J/(kg·K)
5.	UA	Overall heat transfer coefficient of the rector wall	50	W/K
6.	k_{loss}	Heat loss coefficient from the reactor to the environment	2	W/K
7.	R	Universal gas constant	8.314	J/(mol·K)
8.	V_h	Headspace volume inside the reactor	0.01	m^3
9.	V_t	Gas storage tank volume	0.01	m^3
10.	P_{heat}	Maximum thermal power of the heating actuator	1000	W
11.	C_v	Flow coefficient of the solenoid valve	10^{-15}	$mol/(s \cdot \sqrt{Pa})$
12.	Q_{rxr}	Heat of metabolic reaction from yeast	10	W
13.	T_{amb}	Ambient air temperature	298	K
14.	F_{gas}	CO_2 gas production rate from the fermentation process	10^{-4}	mol/s

Source: Computational Results and Tool Characterization

3.2. System Linearization

The mathematical model of the bioreactor is non-linear, comprising the state vector $\mathbf{x} = \left[T, T_j, P_r, P_g\right]^T$ and the input vector $\mathbf{u} = [u_h, u_v]^T$. Assuming all state variables are fully measurable, the output matrix is defined as an identity matrix ($y = x$). To implement the LTV-MPC algorithm, the system's dynamic equation $\dot{\mathbf{x}}(t) = f(\mathbf{x}(t), \mathbf{u}(t), t)$ is linearized using a first-order Taylor series expansion (Villarreal et al., 2022).

The operating point is evaluated at each sampling time k based on the state-space conditions (x_k, u_{k-1}), yielding a time-varying local linear deviation equation:

$$\dot{\tilde{\mathbf{x}}} \approx \boldsymbol{A}_{cl}(k)\tilde{\mathbf{x}}(t) + \boldsymbol{B}_{cl}(k)\tilde{\mathbf{u}}(t) \quad (7)$$

The dynamic matrix $A_{cl}(k)$ and the input matrix are computed by Jacobian operation:

$$\boldsymbol{A}_{cl}(k) = \left.\frac{\partial f}{\partial x}\right|_{\mathbf{x}=\mathbf{x}_k, \mathbf{u}=\mathbf{u}_k, t=t_k}, \qquad \boldsymbol{B}_{cl}(k) = \left.\frac{\partial f}{\partial u}\right|_{\boldsymbol{x}=\boldsymbol{x_k}, \boldsymbol{u}=\boldsymbol{u_k}, \boldsymbol{t}=\boldsymbol{t_k}} \quad (8)$$

Evaluating these Jacobians at each sampling interval yields the following

https://doi.org/10.30736/voj.v8i2.1367

E-ISSN: 2656-5846
P-ISSN: 2656-2286

time-varying matrices:

$$\boldsymbol{A}_{cl} = \begin{bmatrix} -\frac{UA}{m_r C_{p,r}} & \frac{UA}{m_r C_{p,r}} & 0 & 0 \\ \frac{UA}{m_j C_{p,j}} & -\frac{UA+k_{loss}}{m_j C_{p,j}} & 0 & 0 \\ \frac{R}{V_h}\left(F_{gas}-\beta\right)-\frac{P_r}{T^2}\mu_{clo} & \frac{P_r UA}{T m_r C_{p,r}} & -\frac{T}{V_h}\lambda+\delta-\frac{UA}{m_r C_{p,r}} & \frac{T}{V_h}\lambda \\ 0 & 0 & \frac{T_{amb}}{V_t}\lambda & -\frac{T_{amb}}{V_t}\lambda \end{bmatrix} \tag{9}$$

$$\boldsymbol{B}_{cl} = \begin{bmatrix} \frac{P_{heat}}{m_r C_{p,r}} & 0 \\ 0 & 0 \\ \frac{P_r P_{heat}}{T m_r C_{p,r}} & -\frac{RT}{V_h} C_v u_v \sqrt{P_r - P_g} \\ 0 & \frac{RT_{amb}}{V_t}\left(C_v u_v \sqrt{P_r - P_g}\right) \end{bmatrix} \tag{10}$$

The auxiliary variables,

$$\mu_{clo} = \frac{u_h P_{heat} + Q_{rxr} + UAT_j}{m_r C_{p,r}}, \qquad \delta = \frac{\mu_{clo}}{T}$$

$$\beta = C_v u_v \sqrt{P_r - P_g}, \qquad \lambda = R C_v u_v \frac{1}{2\sqrt{P_r - P_g}}$$

3.3. Discretization

The design of the LTV-MPC requires a prediction model in the discrete-time domain. The continuous-time model obtained from linearization at the k-th interval is expressed as.

$$\dot{\mathbf{x}}(t) = \boldsymbol{A}_{cl}(t)\mathbf{x}(t) + \boldsymbol{B}_{cl}(t)\mathbf{u}(t) \tag{11}$$

Discretization is carried out using a piecewise-constant approach, in which the system matrices are assumed to remain constant over one sampling period, so that $\boldsymbol{A}_{cl,k} = \boldsymbol{A}_{cl}(t_k)$ and $\boldsymbol{B}_{cl,k} = \boldsymbol{B}_{cl}(t_k)$. This is combined with a zero-order hold (ZOH) assumption, which keeps $\mathbf{u}(t) = \mathbf{u}_k$ for $t \in [t_k, t_k + \Delta t]$. Under these assumptions, solving (11) over the k-th interval yields the discrete-time model

$$\mathbf{x}_{k+1} = \boldsymbol{A}_{d,k}\mathbf{x}_k + \boldsymbol{B}_{d,k}\mathbf{u}_k \tag{12}$$

where $\boldsymbol{A}_{d,k} = e^{\boldsymbol{A}_{cl,k}\Delta t}$ and $\boldsymbol{B}_{d,k} = \int_0^{\Delta t} e^{\boldsymbol{A}_{cl,k}(\Delta t-\tau)}\boldsymbol{B}_{cl,k}d\tau$. Computationally, both matrices are obtained simultaneously through the exponential of the augmented matrix

$$\exp\left(\begin{bmatrix} \boldsymbol{A}_{cl,k} & \boldsymbol{B}_{cl,k} \\ 0 & 0 \end{bmatrix}\Delta t\right) = \begin{bmatrix} \boldsymbol{A}_{cl,k} & \boldsymbol{B}_{cl,k} \\ 0 & \boldsymbol{I} \end{bmatrix} \tag{13}$$

so that the convolution integral in $\boldsymbol{B}_{d,k}$ need not be evaluated analytically.

Since the MPC cost function penalizes the input increment $\Delta\mathbf{u}_k = \mathbf{u}_{k-1}$ to prevent abrupt changes in the heater and valve actions, model (13) is extended using the augmented state vector $\mathbf{X}_k = \begin{bmatrix} \boldsymbol{x_k^T} & \boldsymbol{u}_{k-1}^T \end{bmatrix}^T$, which gives

$$\begin{bmatrix} \mathbf{x}_{k+1} \\ \mathbf{u}_k \end{bmatrix} = \begin{bmatrix} \boldsymbol{A}_{d,k} & \boldsymbol{B}_{d,k} \\ 0_{2\times 4} & \boldsymbol{I}_{2\times 2} \end{bmatrix}\begin{bmatrix} \mathbf{x}_k \\ \mathbf{u}_{k-1} \end{bmatrix} + \begin{bmatrix} \boldsymbol{B}_{d,k} \\ \boldsymbol{I}_{2\times 2} \end{bmatrix}\Delta\mathbf{u}_k \tag{14}$$

For the bioreactor, with $\mathbf{x}_k = [T \quad T_j \quad P_r \quad P_g]^T$ and $\boldsymbol{u}_k = [u_h \quad u_v]^T$, the augmented state vector has dimension 6×1, and (14) serves as the prediction

E-ISSN: 2656-5846
P-ISSN: 2656-2286

model employed in the LTV-MPC.

3.4. Structural System Property Analysis

3.4.1. Stability Analysis

System stability about the reference trajectory assessed using the state transition matrix of the linearized LTV model. With the Jacobian matrix assumed piecewise constant over each sampling interval, $\boldsymbol{A}(t) \approx \boldsymbol{A}_k$ for $t \in [t_k, t_{k+1})$, the local transition matrix is $\boldsymbol{\Phi}(t_{k+1}, t_k) = e^{\boldsymbol{A}_k \Delta t}$, and the global matrix follows from the ordered product $\boldsymbol{\Phi}(t_N, t_0) = \boldsymbol{\Phi}(t_N, t_{N-1}) \ldots \boldsymbol{\Phi}(t_1, t_0)$, the ordering being preserved because LTV system are non-commutative in time.

Stability id then judged form its induced 2-norm, $\gamma_k = \left|\left|\boldsymbol{\Phi}(t_k, t_0)\right|\right|_2$, the system is Lyapunov stable if $\gamma_k \leq M$ for some finite M, and unstable if γ_k grows monotonically without bound.

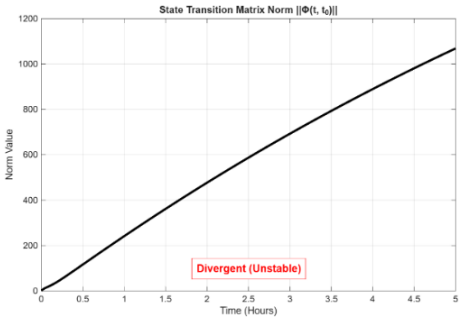


Figure 2. Stability Analysis Results

As shown in Figure 2, the monotonic growth to an order of 10^3 over the 5-hour horizon indicates system instability with no finite bound. Since these amplified perturbations risk pressure runaway, LTV-MPC to maintain safe operation.

3.4.2. Controllability and Observability Analysis

The structural properties of the system are examined using the Gramian approach, which remains valid for time varying system. With $\boldsymbol{\Phi}(t, t_0)$ denoting the state transiton matrix,

$$\boldsymbol{W_o}(t_0, t_f) = \int_{t_0}^{t_f} \boldsymbol{\Phi}^T(t, t_0) \mathbf{C}^{\mathrm{T}} \mathbf{C} \boldsymbol{\Phi}(t, t_0) dt \tag{15}$$

$$\boldsymbol{W_c}(t_0, t_f) = \int_{t_0}^{t_f} \boldsymbol{\Phi}(t_f, t) \boldsymbol{B}(t) \boldsymbol{B}^T \boldsymbol{\Phi}^T(t_f, t) dt \tag{16}$$

Since $C = \boldsymbol{I}_4$, the observability Gramian reduces to $W_o = \int_{t_0}^{t_f} \boldsymbol{\Phi}^T(t, t_0) \boldsymbol{\Phi}(t, t_0) dt$.

The system is completely observable and controllable over $[t_0, t_f]$ or [0,18000] if

$$\det(\boldsymbol{W_o}) \neq 0 \text{ and } \det(\boldsymbol{W_c}) \neq 0 \tag{17}$$

Numerical evaluation of (1) and (2) in MATLAB over the simulation interval yields,

$$\det(\boldsymbol{W_o}) = 1.3713 \times 10^{16}, \quad \det(\boldsymbol{W_c}) = 12.5262$$

Both determinants are nonzero, so the bioreactor system is completely observable and completely controllable, which justifies the application of LTV-MPC.

3.5. LTV-MPC Control Design

E-ISSN: 2656-5846
P-ISSN: 2656-2286

In this section, the stages of the LTV-MPC control design are described, implemented with a sampling time (T_s) of 60 seconds.

3.5.1. Prediction of State and Output Variables

Future trajectory predictions over the prediction horizon ($N_p = 30$) and control horizon ($N_c = 8$) are derived from the augmented model:

$$\bar{\boldsymbol{Y}} = \boldsymbol{F}\boldsymbol{X}(k) + \boldsymbol{\Phi}\boldsymbol{\Delta}\boldsymbol{U} \tag{18}$$

where $\bar{\boldsymbol{Y}}$ is the predicted output trajectory, $\boldsymbol{X}(k)$ is the current augmented state vector, $\Delta\boldsymbol{U}$ is the vector of actuator action changes, F and $\boldsymbol{\Phi}$ are the free and forced response matrices.

3.5.2. Formulation of the Cost Function

To track setpoints ($50°C$, 145 psi) and suppress actuator surges, the standard MPC cost function:

$$J = \sum_{i=1}^{N_p} \left|\left| y(k+i|k) - r_{ref}(k+i) \right|\right|_{\boldsymbol{Q}}^2 + \sum_{j=0}^{N_c-1} \left|\left| \Delta u(k+j) \right|\right|_{\boldsymbol{R}}^2 \tag{18}$$

is derived into its augmented quadratic matrix form:

$$J = \left(\bar{\boldsymbol{X}} - \bar{\boldsymbol{R}}_{\boldsymbol{ref}}\right)^T \bar{\boldsymbol{Q}} \left(\bar{\boldsymbol{X}} - \bar{\boldsymbol{R}}_{\boldsymbol{ref}}\right) + \Delta\boldsymbol{U}^T \bar{\boldsymbol{R}} \Delta\boldsymbol{U} \tag{19}$$

where $\bar{\boldsymbol{R}}_{\boldsymbol{ref}}$ is the augmented reference trajectory vector, and $\bar{\boldsymbol{Q}}$ and $\bar{\boldsymbol{R}}$ are block diagonal matrices repeating the base weighting matrices $\boldsymbol{Q}$ and $\boldsymbol{R}$ along their diagonals. Utilizing Bryson's Rule (Xiao et al., 2026), the base matrices are tuned to.

$$\boldsymbol{Q} = diag([5000, 10, 50, 1]), \quad \boldsymbol{R} = diag([100, 0.05]) \tag{20}$$

high weights on palm sap temperature ($q_1 = 5000$) and heating power ($r_1 = 100$) are applied to dampen the thermal lag effect, while a low weight on the gas valve ($r_2 = 0.05$) aims to provide an aggressive response to gas pressure surges.

3.5.3. Implementation of Constraints

The LTV-MPC algorithm is subject to a set of operational constraints represented in the form of linear matrix inequalities. The physical constraints applied to this system include:

a. Input constraints
   Both inputs are bounded to a $0\% - 100\%$ operating range: $0 \leq u_h(k) \leq 1$ for heater power and $0 \leq u_v(k) \leq 1$ for the gas valve opening.
b. Increment Constraints
   To prevent extreme oscillations, the rate of change for the actuators is limited. The heating power is restricted to a maximum of $\pm 10\%$ per minute ($-0.1 \leq \Delta u_h \leq 0.1$), and the gas valve to a maximum of $\pm 50\%$ per minute ($-0.5 \leq \Delta u_v \leq 0.5$).
c. State and Output Constraints
   Limiting internal variable fluctuations to ensure the system does not reach critical limits of overheating or overpressure during the fermentation process.

3.6. LTV-MPC Simulation

Utilizing the previously defined horizons (N_p, N_c) and weighting matrices (Q, R), the simulation focuses on tracking the juice temperature (50°) and reactor pressure (145 psi) setpoints. Performance is evaluated by output accuracy, actuator smoothness, and overpressure prevention. The flowchart of the LTV-MPC process

E-ISSN: 2656-5846
P-ISSN: 2656-2286

can be seen in Figure 3.

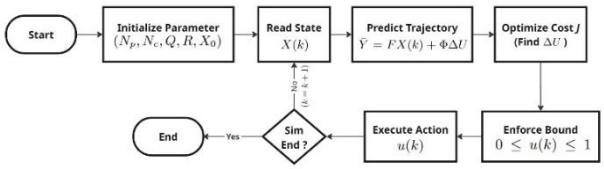


Figure 3. Flowchart of The LTV-MPC Simulation Process

3.6.1. LTV-MPC Simulation Results Analysis

a. Heater control signal analysis

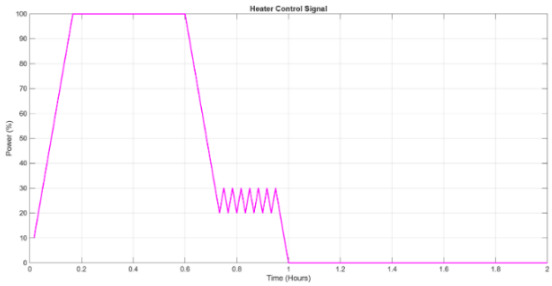


Figure 4. Heater Control Signal

During the first 35 minutes, the heater operated at 100% capacity before dropping to 20% to prevent pressure surges beyond 145 psi. Between minutes 42 and 57 (x = 0.7 to 0.95 hours), power fluctuated between 20% and 30% to track the 43°C setpoint. Importantly, this high-frequency chattering is not a plotting artifact, solver error, or step-size issue. Instead, it reflects the actual LTV-MPC control action dynamically maintaining strict thermal equilibrium without violating safety constraints, before completely shutting off at minute 60. Rapid modulation matches heat transfer to bioreactor dynamics, preventing critical overpressure.

b. Bioreactor temperature response analysis

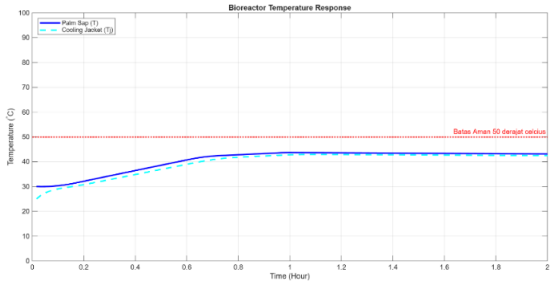


Figure 5. Temperature Response

The temperature rose gradually from 30°C to a stable 43.7°C by minute 60. Its smooth trajectory, despite sharp heater oscillations, stems from the high thermal inertia of the 40 kg palm sap. This equilibrium safely balances the exothermic yeast metabolism and environmental heat loss below the 50°C limit. The 43.7°C deviation is a deliberate $\boldsymbol{Q/R}$ matrix optimization trade-off, prioritizing the 145 psi pressure limit over strict temperature tracking. This reflects optimal predictive prioritization rather than actuator saturation; the heater dynamically modulated between 20% and 30%, operating safely within

E-ISSN: 2656-5846
P-ISSN: 2656-2286

the explicit $0 \leq u_h(k) \leq 1$ bounds without saturating at absolute limits.

c. Gas valve control signal analysis

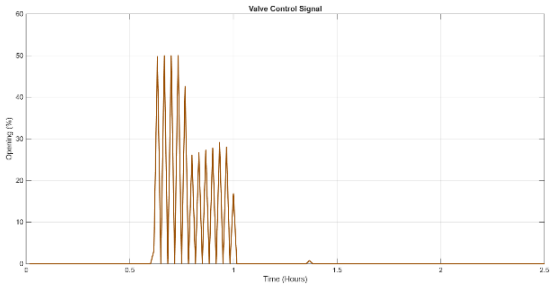


Figure 6. Valve Control Signal

During the first 35 minutes, the valve remained closed before rapidly fluctuating between 0% and 50% until minute 60. This emergency maneuver released excess gas (162 psi) while preventing pressure from dropping below 145 psi. To clarify the applied constraints, the presented figures explicitly illustrate the absolute system inputs (u), which are bounded by $0 \leq u_v(k) \leq 1$. Although the LTV-MPC cost function penalizes the input increment (Δu) the boundaries enforced and plotted in this simulation specifically correspond to the absolute physical saturation limits of the actuators (u).

d. Analysis of reactor and storage tank pressure response

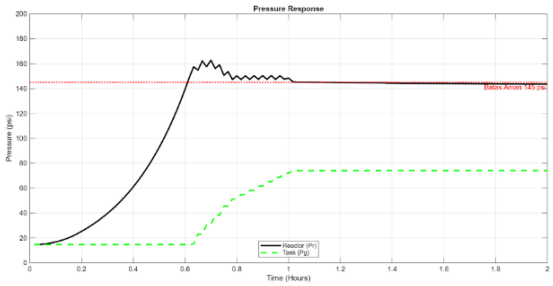


Figure 7. Pressure Response

The pressure inside the reactor initially surged sharply beyond the safety limit, reaching its highest overshoot peak at 162.76 psi at minute 36. Starting from minute 41, the pressure graph began to display an intense oscillatory pattern. This pattern physically represented a recurring cycle: a pressure drop caused by the gas release through the valve, followed by a pressure rise as the yeast in the heated liquid continued to produce expanding CO2 gas. Gradual gas release dampened fluctuations and stabilized pressure at 145 psi within 60 minutes.

4. Conclusions

This study successfully developed and implemented a Linear Time-Varying Model Predictive Control (LTV-MPC) strategy to regulate the simultaneous thermal and hydrodynamic dynamics of a fermentation bioreactor. The derived mathematical framework accurately captured the system by mapping the four state variables and two manipulated inputs into a discrete augmented state-space model via successive Jacobian linearization. Closed-loop simulations confirmed that the LTV-MPC algorithm effectively tracked the critical operational setpoints

E-ISSN: 2656-5846
P-ISSN: 2656-2286

of 50°C for the reactor and jacket temperatures, and 145 psi for the reactor and gas storage tank pressures.

Furthermore, the control actions eliminated steady-state errors, ensured trajectory stability, and respected actuator constraints. Consequently, this control scheme promotes safe, efficient fermentation while reducing risks of thermal accumulation and overpressure. Future research should investigate robust or stochastic MPC to mitigate unmeasured external disturbances during real-time operations.

Author Contributions

Aisyah Fikriyah Zahirah: Conceptualization, Methodology, Formal analysis, Writing - original draft. Dia Ayu Nazihah: Formal analysis and Writing - original draft and Writing - editing. Ni Luh De Siska Sari Dewi: Data curation and Writing - editing. Arief Abdurrakhman: Data curation and Visualization. Mardlijah Mardlijah: Promotor, Methodology, Supervision, Validation, Writing - review.

Acknowledgment

The authors express their sincere gratitude to the Department of Mathematics, FSAD, Institut Teknologi Sepuluh Nopember, for its invaluable support, technical guidance, and provision of laboratory facilities throughout this bioethanol bioreactor study.

Declaration of Competing Interest

There is no conflict of interest in writing this article.

References

Ameliyah, A. N., & Arif, D. K. (2026). Estimation of Dengue Fever Transmission Model in West Java Using the Ensemble Kalman Filter Method. *Vygotsky*, *8*(1), 51–64. https://doi.org/10.30736/voj.v8i1.1325

Bujarbaruah, M., Rosolia, U., Stürz, Y. R., Zhang, X., & Borrelli, F. (2022). Robust MPC for LPV Systems Via A Novel Optimization-Based Constraint Tightening. *Automatica*, *143 110459*. https://doi.org/10.1016/j.automatica.2022.110459

Darajat, P. P., Cipta, B. S. I., Nuruddin, I. F., & Balqis, D. A. I. (2023). Dynamical Analysis and Optimal Control of SVIR Hepatitis B Model Spread in Malang. *Vygotsky*, *5*(2), 77. https://doi.org/10.30736/voj.v5i2.698

Deloitte Consulting Southeast Asia. (2023). *Study on Policy Advocacy for Biofuel in Indonesia: Final Report*. https://www.nedo.go.jp/content/800017454.pdf

Dewi, D. S., Hiya, N., Rajali, M., & Harahap, S. K. (2024). Budidaya Pohon Aren di Siopat Sosor Parbaba Samosir Tapanuli Utara. *Jurnal Abdimas UPMI*, *3*(1), 17–23.

Dewi, Ni Luh De Siska Sari, Zahirah, A. F., Nazihah, D. A., Abdurrakhman, A., & Mardlijah, M. (2026). Modeling and Implementation of Linear Time-Varying Model Predictive Control (LTV-MPC) for A Distillation System. *Journal Focus Action of Research Mathematic (Factor M)*, *9*(1), 79–94. https://doi.org/10.30762/f_m.v9i1.8490

Hutami, R., Pribadi, M. F. I., Nurcahali, F., Septiani, B., Andarwulan, N., Sapanli, K., Zuhud, E. A. M., Al Manar, P., Ichsan, N., & Wahyudi, S. (2023). Proses Produksi Gula Aren Cetak (Arenga Pinnata, Merr) di Indonesia. *Jurnal Ilmiah Pangan Halal*, *5*(2), 119–130. https://doi.org/10.30997/jiph.v5i2.10237

E-ISSN: 2656-5846
P-ISSN: 2656-2286

Khairiah, H., & Ridwan, M. (2021). Pengembangan Proses Pembuatan Bioetanol Generasi II dari Limbah Tandan Kosong Kelapa Sawit. *Jurnal Pangan Dan Agroindustri*, *9*(4), 233–240. https://doi.org/10.21776/ub.jpa.2021.009.04.5

Krisnanto, W., Riska Nurfaila, & Muhammad anshori. (2025). Kualitas Bioetanol Tuak Tuban dari Nira Siwalan (Borassus Flabellifer Linn) dengan Metode Fermentasi sebagai Bahan Bakar Alternatif. *Journal of Mechanical Engineering and Applied Technology (JMEAT)*, *3*(1), 25–30. https://doi.org/10.32497/jmeat.v3i1.6505

Kumar, M., Prasad, D., Giri, B. S., & Singh, R. S. (2019). Temperature Control of Fermentation Bioreactor for Ethanol Production Using IMC-PID Controller. *Biotechnology Reports*, *22*, e00319. https://doi.org/10.1016/j.btre.2019.e00319

Ławryńczuk, M., Marusak, P. M., Chaber, P., & Seredyński, D. (2022). Initialisation of Optimisation Solvers for Nonlinear Model Predictive Control: Classical vs. Hybrid Methods. *Energies*, *15*(7), 2483. https://doi.org/10.3390/en15072483

Nadal-Rey, G., McClure, D. D., Kavanagh, J. M., Cornelissen, S., Fletcher, D. F., & Gernaey, K. V. (2021). Understanding Gradients in Industrial Bioreactors. *Biotechnology Advances*, *46 107660*. https://doi.org/10.1016/j.biotechadv.2020.107660

Rifa'i, A. F., Pamungkas, W. A., Setyawati, R. B., Setiawan, C. P., & Waluyo, J. (2022). Kajian Teknoekonomi Bioetanol Berbahan Molasses sebagai Alternatif Substitusi BBM. *Equilibrium Journal of Chemical Engineering*, *6*(1), 61. https://doi.org/10.20961/equilibrium.v6i1.63158

Salazar, Y., Valle, P. A., Rodríguez, E., Soto-Cruz, N. O., Páez-Lerma, J. B., & Reyes-Sánchez, F. J. (2023). Mechanistic Modelling of Biomass Growth, Glucose Consumption and Ethanol Production by Kluyveromyces Marxianus in Batch Fermentation. *Entropy*, *25*(3), 497. https://doi.org/10.3390/e25030497

Villarreal, Gonzalez Oscar Julian, Rossiter, J. A., & Tsourdos, A. (2022). An Efficient Condensing Algorithm for Fast Closed Loop Dual-Mode Nonlinear Model Predictive Control. *IET Control Theory & Applications*, *16*(9), 872–888. https://doi.org/10.1049/cth2.12274

Wilberta, N., Sonya, N. T., & Lydia, S. H. R. (2021). Analisis Kandungan Gula Reduksi pada Gula Semut dari Nira Aren yang Dipengaruhi pH dan Kadar Air. *Bioedukasi (Jurnal Pendidikan Biologi)*, *12*(1), 101–108. https://doi.org/10.24127/bioedukasi.v12i1.3760

Xiao, Y., Lei, J., Qin, X., Wei, C., Lu, L., Wang, S., & Wang, C. (2026). ISO-Optimized Quantile Regression LSSVM-Based Adaptive Robust MPC for Forward Speed Control of Pepper Harvesters. *Smart Agricultural Technology*, *14 102055*. https://doi.org/10.1016/j.atech.2026.102055

Xu, S., Bai, J., & Zou, H. (2026). Improved design of Constrained Model Predictive Tracking Control for Industrial Processes Against Unknown Uncertainties and Partial Actuator Failure. *The Canadian Journal of Chemical Engineering*, *104*(9), 4946–4956. https://doi.org/10.1002/cjce.70317

Zhang, Jian, Xu, Y., & Li, Y. (2025). An Improved State Space Model Predictive Control for Linear Systems with Input Disturbance. *Transactions of the Institute of Measurement and Control*, *47*(1), 51–61. https://doi.org/10.1177/01423312241241361

Zhang, X., Sun, J., & Wang, G. (2023). State and Input Observability of Multi-Agent Aystems: A Necessary and Sufficient Condition. *Systems & Control Letters*, *181 105647*. https://doi.org/10.1016/j.sysconle.2023.105647